Probing charge transfer characteristics in a donor–acceptor metal–organic framework by Raman spectroelectrochemistry and pressure-dependence studies

Usov, P. M.; Leong, C. F.; Chan, B.; Hayashi, M.; Kitagawa, H.; Sutton, J. J.; Gordon, K. C.; Hod, I.; Farha, O. K.; Hupp, J. T.; Addicoat, M.; Kuc, A. B.; Heine, T.; D'Alessandro, D. M.;

Originally published:

September 2018

Physical Chemistry Chemical Physics 20(2018)40, 25772-25779

DOI: https://doi.org/10.1039/C8CP04157A

Perma-Link to Publication Repository of HZDR:

https://www.hzdr.de/publications/Publ-28003

PCCP

Accepted Manuscript

ROYAL SOCIETY OF CHEMISTRY

rsc.li/pccp

View Article Online
DOI: 10.1039/C8CP04157A

Probing charge transfer characteristics in a donor–acceptor metal-organic framework by Raman spectroelectrochemistry and pressure-dependence studies

Pavel M. Usov[a], Chanel F. Leong[a], Bun Chan[a,b], Mikihiro Hayashi[c], Hiroshi Kitagawa[c], Joshua J. Sutton[d], Keith C. Gordon[d], Idan Hod[e], Omar K. Farha[e], Joseph T. Hupp[e], Matthew Addicoat[f,g], Agnieszka Beata Kuc[g,h], Thomas Heine[g,h,i], Deanna M. D'Alessandro[a]*

[a] *School of Chemistry, The University of Sydney, New South Wales 2006, Australia*

[b] *Graduate School of Engineering, Nagasaki University, Bunkyo 1-14, Nagasaki 852-8521, Japan*

[c] *Division of Chemistry, Graduate School of Science, Kyoto University 606-8501, Japan*

[d] *Department of Chemistry, University of Otago, Dunedin 9016, New Zealand*

[e] *Department of Chemistry, Northwestern University, Evanston, Illinois 60208-3113, USA*

[f] *School of Science and Technology, Nottingham Trent University, UK*

[g] *Wilhelm-Ostwald-Institute for Physical and Theoretical Chemistry, Universität Leipzig, Germany*

[h] *Helmholtz Center Dresden-Rossendorf, Institute of Resource Ecology, Leipzig Branch, Permoserstr. 15 | D-04318 Leipzig | Germany*

[i] *School of Science, Faculty of Chemistry and Food Chemistry, TU Dresden, Mommsenstr. 13, 01062 Dresden, Germany*

ABSTRACT

The stimuli responsive behaviour of charge transfer donor-acceptor metal-organic frameworks (MOFs) remains an understudied phenomenon which may have applications in tuneable electronic materials. We now report the modification of donor-acceptor charge transfer characteristics in a semiconducting tetrathiafulvalene-naphthalene diimide-based MOF under applied electrochemical bias and pressure. We employ a facile solid state *in situ* Raman spectroelectrochemical technique, applied for the first time in the characterisation of electroactive MOFs, to monitor the formation of a new complex $TTFTC^{\bullet+}$–DPNI from a largely neutral system, upon electrochemical oxidation of the framework. *In situ* pressure-dependent Raman spectroscopy and powder X-ray diffraction experiments performed in a diamond anvil cell revealed blue shifts in the donor and acceptor vibrational modes in

View Article Online
DOI: 10.1039/C8CP04157A

addition to contractions in the unit cell which are indicative of bond shortening. This study demonstrates the utility of *in situ* Raman spectroscopic techniques in the characterisation of redox-active MOFs and the elucidation of their electronic behaviours.

INTRODUCTION

The rapidly expanding fields of electroactive and conductive Metal-Organic Frameworks (MOFs) and coordination polymers (CPs) have provided fundamentally new insights into charge transfer interactions in three-dimensional materials.[1-4] Spectroscopic investigations have proven particularly useful to probe the relationship between the optical and electronic properties of framework materials and elucidate mechanisms of charge transport in extended coordination space.[2, 5-7] A deeper understanding of the electronic properties of MOFs and CPs will enable the targeted design of materials that are relevant to real-world device applications.[8, 9]

MOFs that incorporate donor–acceptor (D–A) components exhibit unique charge transfer characteristics which have been shown to promote charge transfer pathways that facilitate electrical conductivity.[4, 10-12] The area of D–A MOFs has been inspired in major part by the rich literature on organic charge transfer complexes whereby the archetypal 'organic metal' tetrathiafulvalene-tetracyanoquinodimethane (TTF–TCNQ) demonstrated a conductivity comparable to metallic copper.[13] Apart from their often intrinsically conductive properties, organic charge transfer complexes have been shown to undergo neutral-ionic phase transitions upon application of external stimuli, such as temperature, pressure and light.[14] The exploration of such electronic modifications, largely by electrochemical and pressure-induced changes, remains extremely limited in D–A MOFs. Such external stimuli hold immense promise as additional handles to modify and switch the electronic properties.

Spectroscopic techniques including infrared (IR) and Raman spectroscopies are ideal characterisation tools to explore switchable properties given the sensitivity of molecular vibrations to the structural and electronic characteristics of molecules. Raman spectroscopy has been applied to probe the oxidation states of numerous redox-active moieties such as tetrathiafulvalene (TTF)[15-17] and tetracyanoquinodimethane (TCNQ)[18, 19] owing to the change in bond order upon redox state changes. Raman spectroelectrochemistry (SEC) has been extensively utilised for the investigation of spectroscopic changes associated with redox transformations in soluble discrete and thin-film systems.[20-22] These *in situ* SEC experiments

View Article Online
DOI: 10.1039/C8CP04157A

are typically performed either in transmittance mode using a variation of the optically transparent thin-layer electrochemical (OTTLE) cell,[23] or in reflectance mode in conjunction with a confocal microscope.[24] The added advantage of Raman spectroscopy is resonance enhancement; this involves light excitation into specific electronic transitions which allows insights into electronic structure.[25]

A previous study on the D–A MOF [(Zn(DMF))$_2$(TTFTC)(DPNI)] (DMF = *N,N*-dimethylformamide, TTFTC = tetrathiafulvalene tetracarboxylate and DPNI = *N,N′*-di(4-pyridyl)-1,4,5,8-naphthalenetetracarboxydiimide) reported by our group, demonstrated that the degree of through space charge transfer could be modulated using an electrochemical bias.[26] The structure is comprised of mixed stacks of donor TTFTC and acceptor DPNI ligands down the crystallographic *a*-axis (Figure 1). Although Raman spectroscopy has been employed as a technique to characterise the redox state of TTF in framework materials, *in situ* Raman SEC experiments, to date, have not been applied to redox-active MOFs. This method stands as a potentially powerful technique to characterise charge transfer behaviour in these multidimensional solid state systems.

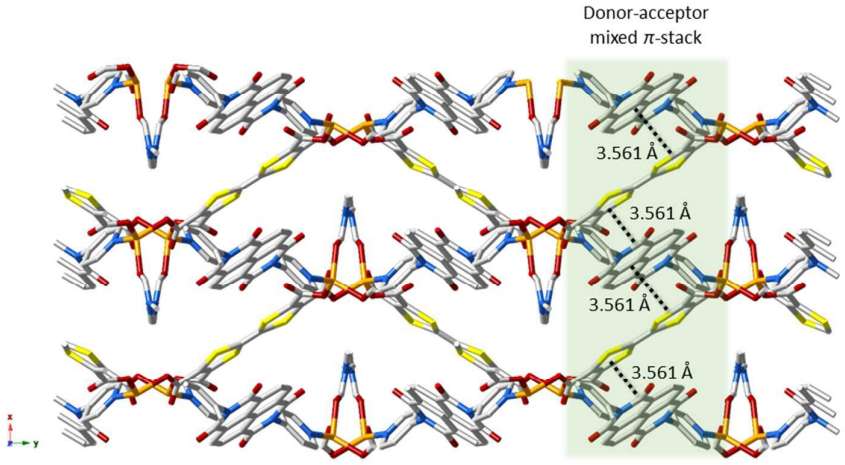

Figure 1. Crystal structure of [(Zn(DMF))$_2$(TTFTC)(DPNI)] viewed down the *c*-axis with the D–A mixed stack highlighted in green.

Additionally, the coupling of Raman spectroscopy with an external stimulus such as pressure can be used to probe the effect of such external stimuli on the charge transfer characteristics of redox-active framework materials. Pressure-induced neutral–ionic transitions have previously been observed in organic charge transfer (CT) complexes and 1D chains, whereby lattice deformations as a result of increased pressure give rise to changes in the electronic

View Article Online
DOI: 10.1039/C8CP04157A

structure and conductive properties.[14] This phenomenon remains unexplored in electroactive MOFs, and high pressure studies may provide important insights into charge transfer behaviours in these materials.

Herein, we report a combined experimental and computational approach to the donor–acceptor (D–A) framework, [(Zn(DMF))$_2$(TTFTC)(DPNI)], which displays partial through-space ligand-to-ligand charge transfer.[26] The development of a new *in situ* solid state Raman spectroelectrochemical (SEC) method to interrogate this electroactive MOF has revealed changes in the vibrational features of the redox-active ligands TTFTC and DPNI under applied potential. This study sheds light on local structural changes brought about by redox modulation which have been corroborated using Density Functional Theory (DFT) calculations. Variable-pressure Raman spectroscopy on [(Zn(DMF))$_2$(TTFTC)(DPNI)] was also employed using a diamond anvil cell (DAC) to provide insights into the influence of pressure on the charge transfer interactions in D–A MOFs. Band structure calculations have also been employed to elucidate the mechanism for charge transport in the material.

EXPERIMENTAL

Synthesis of [(Zn(DMF))$_2$(TTFTC)(DPNI)]. Bulk powder and single crystals of [(Zn(DMF))$_2$(TTFTC)(DPNI)] were synthesised according to a previously reported method (Figure S3).[26]

Raman Spectroscopy. Raman spectra of solid MOF powder on a silicon crystal substrate were measured using an inVia Renishaw Raman microscope under 785 nm laser excitation.

Steady State Resonance Raman Spectroscopy. The spectrum obtained under 406 nm excitation was collecting using an Isoplane SCT320 spectrometer equipped with a Pylon CCD (Princeton Instruments) and a krypton ion laser (Innova 300C, Coherent Scientific Ltd.) The 1064 nm spectrum was measured using a WP1064 Raman spectrometer (Wasatch Photonics).

***In Situ* Solid State Raman Spectroelectrochemistry.** The spectroelectrochemical experiments were performed using DS-150 screen-printed electrodes (DropSens) as the basis for the electrochemical cell (Figure S1). The working electrode consisted of a glassy carbon disc (diameter 4 mm) with a Pt strip used as the counter electrode and Ag plate as the

View Article Online
DOI: 10.1039/C8CP04157A

reference. The screen-printed electrode was placed into the plastic holder (Figure S2) and attached to the microscope plate using insulating tape. The electrical contacts on the electrode were extended by soldering Ag wires. The powdered samples were mechanically immobilised onto the working electrode and a droplet of electrolyte (0.2 M $LiClO_4$/ethylene glycol) added on top. The laser (785 nm) was focused onto the sample through the electrolyte using the Raman microscope (magnification × 10). The Raman spectra were recorded over the 150–2000 cm^{-1} range with 120 s exposure time and 5% laser power.

The potentials were applied using an eDAQ e-corder 410 potentiostat. The potentials of redox processes determined from cyclic voltammetry were used as a guide for the SEC experiment. The potentials were increased in small increments each followed by a spectral measurement. Baseline-correction was performed on the collected data in order to standardise the spectra.

Variable-Pressure Resonance Raman Scattering Spectroscopy. Raman spectra of $[(Zn(DMF))_2(TTFTC)(DPNI)]$ at several pressures were measured using a Micro Laser Raman Spectrometer (NRS-5200; JASCO Corporation) in which a He-Ne laser (λ = 632 nm) was used as the excitation light source. Pressure was applied by use of the diamond anvil cell (DAC) in which Daphne 7474 oil was used as the liquid pressure-transmitting media. In the DAC apparatus, type IIa diamond anvils with 800 μm culets were used. Stainless steel gaskets with 400 μm diameter holes were utilized as the sample compartment. The value of applied pressure was calibrated against the fluorescence of ruby in the sample compartment at each pressure. All experiments were performed at room temperature.

Variable-Pressure Powder X-Ray Diffraction. Pressure dependent powder X-ray diffraction patterns were collected on the 17-BM-B: Rapid Acquisition Powder Diffraction beamline (λ = 0.45212 Å) at the Advanced Photon Source, Argonne National Laboratories, Illinois, U.S.A. The sample was loaded into a stainless steel gasket with a 200 μm diameter hole. Pressure was applied using a Diamond Anvil Cell utilising Fluorinert FC-70 as the pressure-transmitting media and NaCl was used as an internal pressure standard.

Two-point Probe Conductivity. Pellets of powdered sample (approx. 40 mg) were prepared using a pellet press (7.14 mm diameter) at applied pressures of 0.25 tonnes. To the conductive face of two Fluorinated Tin Oxide (FTO) plates of approximate dimensions 3 × 1.5 cm, conductive silver epoxy was applied across the width in 1 cm strips. The pellet was adhered between these two FTO plates ensuring the two faces of the pellet were in complete contact with the silver epoxy. The cell was connected to an AMETEK Solartron Analytical

View Article Online
DOI: 10.1039/C8CP04157A

Modulab Potentiostat and I–V curves were measured over the potential range 3 to −3 V at a sweep rate of 10 mV/s.

Density Functional Theory (DFT) Calculations. Standard DFT calculations were carried out using Gaussian 09.[27] The geometry of the (TTFTC)(DPNI) model was extracted from the crystal structure of the MOF without modification, while discrete TTFTC and DPNI molecules were optimised with the B3-LYP/6-31+G(d,p) procedure.[28] This methodology was chosen because of its robust performance in the prediction of vibrational frequencies.[29-31] Following each geometry optimisation, harmonic frequency analysis was carried out to confirm the nature of the stationary point as an equilibrium structure, as well as to obtain a simulated Raman spectrum. We applied a scale factor of 0.9648 to the vibrational frequencies according to literature recommendations.[28] The degree of charge transfer in the (TTFTC)(DPNI) complex was estimated with Mulliken atomic charges obtained using B3-LYP/6-31+G(d,p) densities. We found that this provides a comparable value to the one reported previously,[26] obtained using densities calculated with a different functional.

Band Structure Calculations. Band structure calculations were performed using density functional theory (DFT) on the optimized systems. The PBE[32] and PBE0[33] exchange-correlation functionals were employed. The all electron TZVP[34] basis sets were used for all atoms. The electron density within the self-consistent calculation was obtained using 40 k-points as a Monkhorst-Pack mesh for MOF structure. The band structure was calculated from the electron density using high-symmetry points and 100 k-points interpolation between them. All calculations were performed using Crystal14 software.[35]

RESULTS AND DISCUSSION

Raman spectroscopy was performed on solid samples of DPNI, H_4TTFTC and [(Zn(DMF))$_2$(TTFTC)(DPNI)] using 785 nm laser excitation, which coincides with the charge transfer transition between the TTFTC donor (TTFTC denotes the fully deprotonated species of H_4TTFTC with a charge of 4− but where TTF is in its neutral state) and DPNI acceptor within the framework.[26] From the resulting spectra (Figure 2), the similarities between the vibrational peaks of the framework and its components are clearly visible. DFT modelling of the vibrational structures of the DPNI^0, DPNI$^{\bullet-}$, TTFTC^0 and TTFTC$^{\bullet+}$ species was used to assign individual peaks which are summarised in Table S1. The Raman spectrum of DPNI^0 was primarily found to contain peaks corresponding to a neutral form, which were assigned to vibrations on the NDI ring system and its carbonyl stretching modes.

View Article Online
DOI: 10.1039/C8CP04157A

Interestingly, the presence of the DPNI radical anion was not detected despite numerous reports on the capacity for NDI-based compounds to generate radicals from light irradiation and the small amount of DPNI radical detected *via* electron paramagnetic resonance (EPR) spectroscopy (Figure S4).[36] In contrast, the vibrational modes corresponding to both neutral and radical forms were observed in the spectrum of H_4TTFTC itself (Figure 2). This is a phenomenon commonly observed in TTF-based compounds owing to both its low oxidation potential and capacity to undergo proton-assisted oxidation.[37] A peak at 500 cm^{-1} was assigned to the S–C stretching mode within the five-membered ring of $TTFTC^{\bullet+}$, whereas peaks at 1404 and 1524 cm^{-1} were attributed to the central C=C stretch of the TTFTC radical cation and symmetric stretching of the outer C=C bonds coupled to the central C=C stretch in neutral TTFTC, respectively.[16] Evidence for the presence of the TTFTC radical cation in the as-synthesised framework $[(Zn(DMF))_2(TTFTC)(DPNI)]$ was found, and is consistent with previous EPR studies on the material.[26]

At 406 nm excitation, peaks attributed to $DPNI^0$ dominate the Raman spectrum of the framework due to excitation of the π-system of the DPNI ligand. At a longer wavelength of 1064 nm, additional peaks at approximately 1500 and 1700 cm^{-1} assigned to C=C of $TTFTC^0$ and C=O of $DPNI^0$, respectively, gain intensity. Thus, excitation into the charge transfer band using 1064 illumination leads to resonance enhancement of the TTFTC and DPNI moieties, both of which play a role in the donor-acceptor charge transfer interaction.

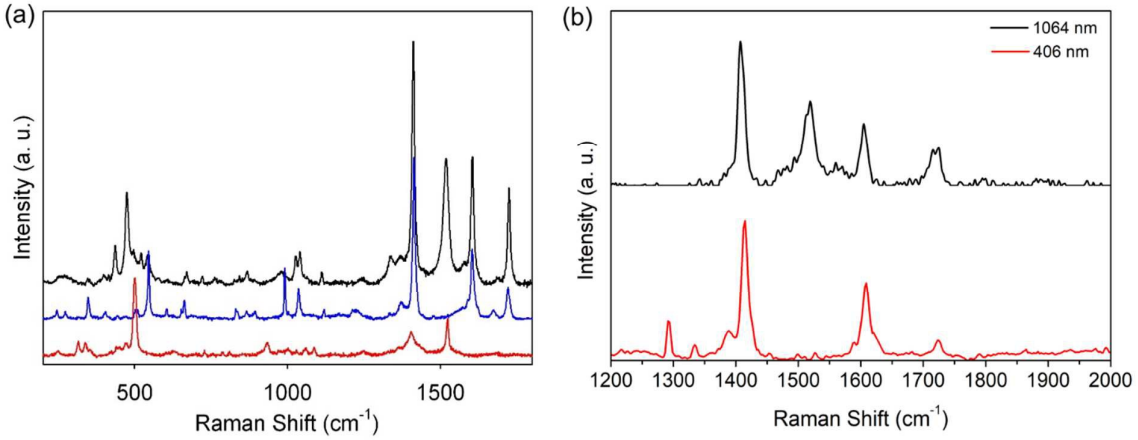

Figure 2. (a) Raman spectra of $[(Zn(DMF))_2(TTFTC)(DPNI)]$ (black), DPNI (blue) and H_4TTFTC (red) under 785 nm laser excitation. (b) Raman spectra of $[(Zn(DMF))_2(TTFTC)(DPNI)]$ obtained under 1064 and 406 nm laser excitation.

View Article Online
DOI: 10.1039/C8CP04157A

The Raman spectrum of [(Zn(DMF))$_2$(TTFTC)(DPNI)] was dominated by DPNI^0, particularly at higher energies (1410, 1605 and 1724 cm^{-1}), as shown in Figure 2. The positions of these peaks did not change significantly between the free ligand and the framework-based ligand, despite its coordination to Zn^{II} centres and π-stacking interactions with adjacent TTFTC units in the latter case. The presence of DPNI^0 species in the framework provides evidence for the heterogeneous nature of charge transfer inside [(Zn(DMF))$_2$(TTFTC)(DPNI)], supporting the results of published work.[26] The consequence of this behaviour, however, is that a portion of the DPNI moiety should exist in a radical form for which no vibrational peaks could be unambiguously identified in the Raman spectrum. It is possible that the intensity of these peaks is low relative to others, and as such, the existence of DPNI$^{\bullet-}$ cannot be ruled out. Two bands corresponding to the TTFTC^0 ligand were identified in the spectrum of the framework at 474 and 1518 cm^{-1}, and were attributed to S–C and C=C stretching bands of TTFTC^0, respectively. On the other hand, the presence of TTFTC$^{\bullet+}$ could not be readily observed even though its existence has been ascertained by UV-vis-NIR and EPR spectroscopies.[26] It is likely that the vibrational peaks for the radical are present in the spectrum but are too low in intensity, similar to that of the DPNI$^{\bullet-}$ species. Overall, Raman spectroscopy has detected the neutral TTFTC and DPNI species within the framework, despite the observation of organic radicals in the framework via EPR spectroscopy. The present results also confirm the heterogeneity of the charge distribution between D and A within the framework.

While recent studies have demonstrated that different measurement techniques have given variable conductivity values for MOFs,[38] the pressed pellet conductivity confirmed the semiconducting nature of [(Zn(DMF))$_2$(TTFTC)(DPNI)]. The room temperature conductivity of the material was measured *via* the 2-point probe method on a pressed pellet. From an I–V curve of the pellet over the range −3 to 3 V, the conductivity was determined to be 2×10^{-5} S cm^{-1} (Figure S5), which is in the range for semiconducting materials. This semiconducting nature is proposed to be facilitated by localised charges within the framework as a result of partial charge transfer from D to A (Scheme 1) in addition to TTFTC radical cations formed by autoxidation of the neutral TTFTC ligand during synthesis as previously shown to occur by EPR studies on the as-synthesised H_4TTFTC (Figure S4).

View Article Online
DOI: 10.1039/C8CP04157A

To understand the charge transfer interactions in $[(Zn(DMF))_2(TTFTC)(DPNI)]$ at a deeper level, band structure calculations were performed (Figure S6). These calculations confirmed the semiconducting nature of the MOF, with an indirect band gap of 1.58 eV (PBE0 level – the less reliable PBE functional predicts a direct band gap of 0.4 eV). In the MOF, the *a* lattice vector corresponds to Γ-X and R-Y, the *b* lattice vector corresponds to X-R, and the *c* lattice vector corresponds to Γ-Z. The band dispersion in the MOF is visible in the top of the valence band, however, the bottom of the conduction band shows almost no dispersion, suggesting that hole transport is the primary mechanism for charge migration in the material. The dispersion between Γ-X and R-Y may correspond to transport along the DPNI linkers, or to transport between DPNI and TTFTC.

In situ Raman Spectroelectrochemistry

The redox state dependence of the vibrational structure of $[(Zn(DMF))_2(TTFTC)(DPNI)]$ was investigated using Raman SEC to determine the effect of electrochemical changes on the charge transfer characteristics. For this purpose, a custom-built solid-state Raman SEC cell was employed using a 0.2 M $LiClO_4$/ethylene glycol supporting electrolyte. As reduction of DPNI causes fluorescence interference (Figure S7), only oxidation of the framework was investigated. The resulting Raman spectra (Figure 3) revealed a considerable spectral change upon application of an anodic potential of 0.4 V. The difference spectrum shown in Figure 3(b) is more instructive with regards to the spectral changes. The bands corresponding to vibrational modes of neutral DPNI increased in intensity uniformly across the entire spectrum; simultaneously, the intensity of peaks attributed to $TTFTC^0$ (477 and 1521 cm^{-1}) decreased in intensity. These spectral changes indicate the presence of two concurrent redox transformations within the framework, namely oxidation of $DPNI^{\bullet-}$ to $DPNI^0$ and $TTFTC^0$ to $TTFTC^{\bullet+}$. The overall process is represented in Scheme 1 where the TTFTC–DPNI π-stack is oxidised giving rise to a new $TTFTC^{\bullet+}$–DPNI CT complex inside the framework. This is consistent with the results from previous DFT modelling of the CT complex which predicted a decrease in the degree of charge transfer (ρ) from 0.6 to 0.2 e^- upon oxidation, due to the higher ionisation potential of $TTFTC^{\bullet+}$ compared to its neutral counterpart, $TTFTC^0$.[26] Although the ρ calculated by DFT is an overestimate of the charge in the system, as demonstrated by Raman spectroscopy and structural characterisation which support a largely neutral system, it successfully accounts for the charge transfer character observed in $[(Zn(DMF))_2(TTFTC)(DPNI)]$. As the applied potential was returned to 0 V, the starting spectrum was not recovered, indicating that the redox transformation was irreversible (Figure

View Article Online
DOI: 10.1039/C8CP04157A

S8). This oxidation process was quasi-reversible on the timescale of the cyclic voltammetry (CV) experiment (i.e., approximately 1 min for CV versus 1 h for SEC), suggesting that the material is less stable to oxidation over the longer timeframe of the SEC experiment. Overall, the oxidation of [$(Zn(DMF))_2$(TTFTC)(DPNI)], which altered the distribution of charge in the MOF, was successfully monitored using Raman SEC and serves as the first example of this technique to be applied to electroactive MOFs.

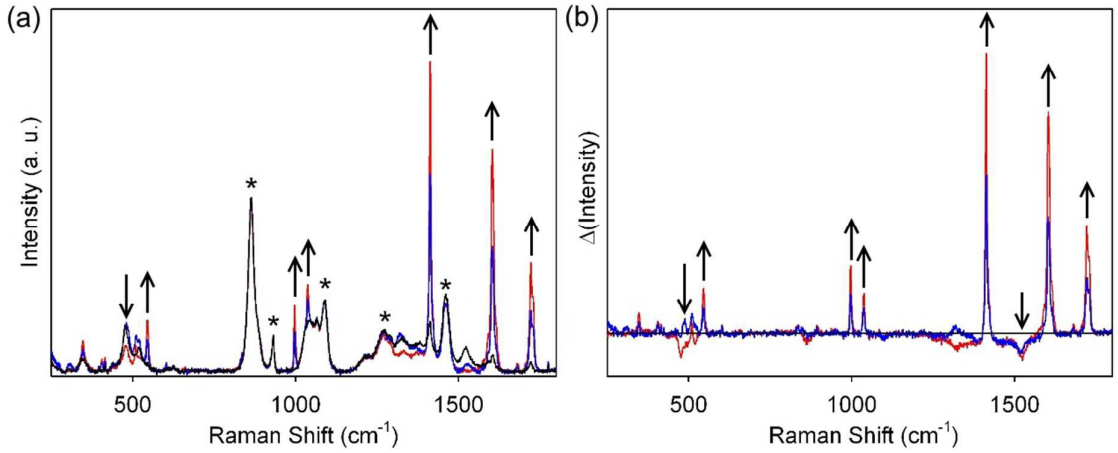

Figure 3. Raman spectrum of [$(Zn(DMF))_2$(TTFTC)(DPNI)] collected on the screen-printed working electrode, using 0.2 M $LiClO_4$/ethylene glycol as a supporting electrolyte, at 0 V (black), 0.2 V (blue) and 0.4 V (red). Arrows denote the direction of spectral change and asterisks denote peaks corresponding to the electrolyte. Spectra were collected under 785 nm laser excitation.

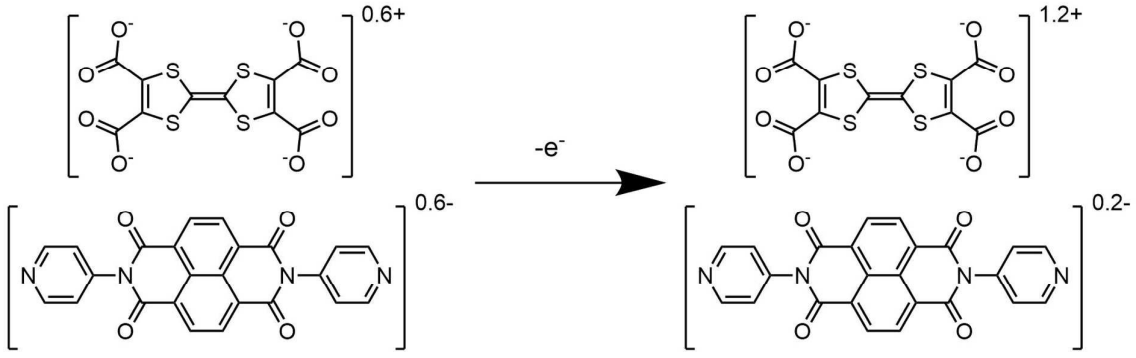

Scheme 1. Proposed oxidation process for DPNI and TTFTC in the [$(Zn(DMF))_2$(TTFTC)(DPNI)] framework.

View Article Online
DOI: 10.1039/C8CP04157A

Pressure-dependent Resonance Raman Scattering Spectroscopy

The sensitivity of charge transfer transitions to external stimuli such as pressure has been explored in a plethora of discrete systems such as organic charge transfer complexes due to the onset of structure changes, new ground states and Peierls distortions.[39, 40] To date, high-pressure studies on MOFs and CPs have uncovered unprecedented structural phase transitions[41] and intermetallic charge transfer,[42] in addition to piezochromism in 1D systems whereby increased pressure has been shown to induce changes in the coordination geometry of the metal ion.[43, 44] The effect of pressure on ligand-based charge transfer characteristics, and the possibility of pressure-induced N–I transitions in donor-acceptor framework materials, however, remains largely unexplored, thus spiking our interest in investigating potential pressure-dependent changes in [$(Zn(DMF))_2$(TTFTC)(DPNI)].

Pressure-dependent Raman spectroscopy (Figure 4(a) and (b)) was performed on a single crystal of [$(Zn(DMF))_2$(TTFTC)(DPNI)] in a diamond anvil cell (DAC), employing ruby as an internal pressure standard and Daphne 7474 as a pressure medium. Spectra were collected over a pressure range of 0–3 GPa. A monotonic blue shift in the peak position (Figure 4(c)) associated with the TTFTC (antisymmetric stretching of the outer C=C bond coupled with the central C=C stretch found at 1600 cm^{-1} and S–C at 500 cm^{-1}) and DPNI (C=O at 1700 cm^{-1}) vibrational modes was observed; this is consistent with bond shortening upon compression of the material which is in line with the unit cell contractions determined by high pressure PXRD (*vide infra*). The absence of any abrupt changes in the spectra with pressure suggests the absence of N–I phase transitions which would be expected to result in non-linear energy shifts in the vibrational modes associated with TTFTC and DPNI.

View Article Online
DOI: 10.1039/C8CP04157A

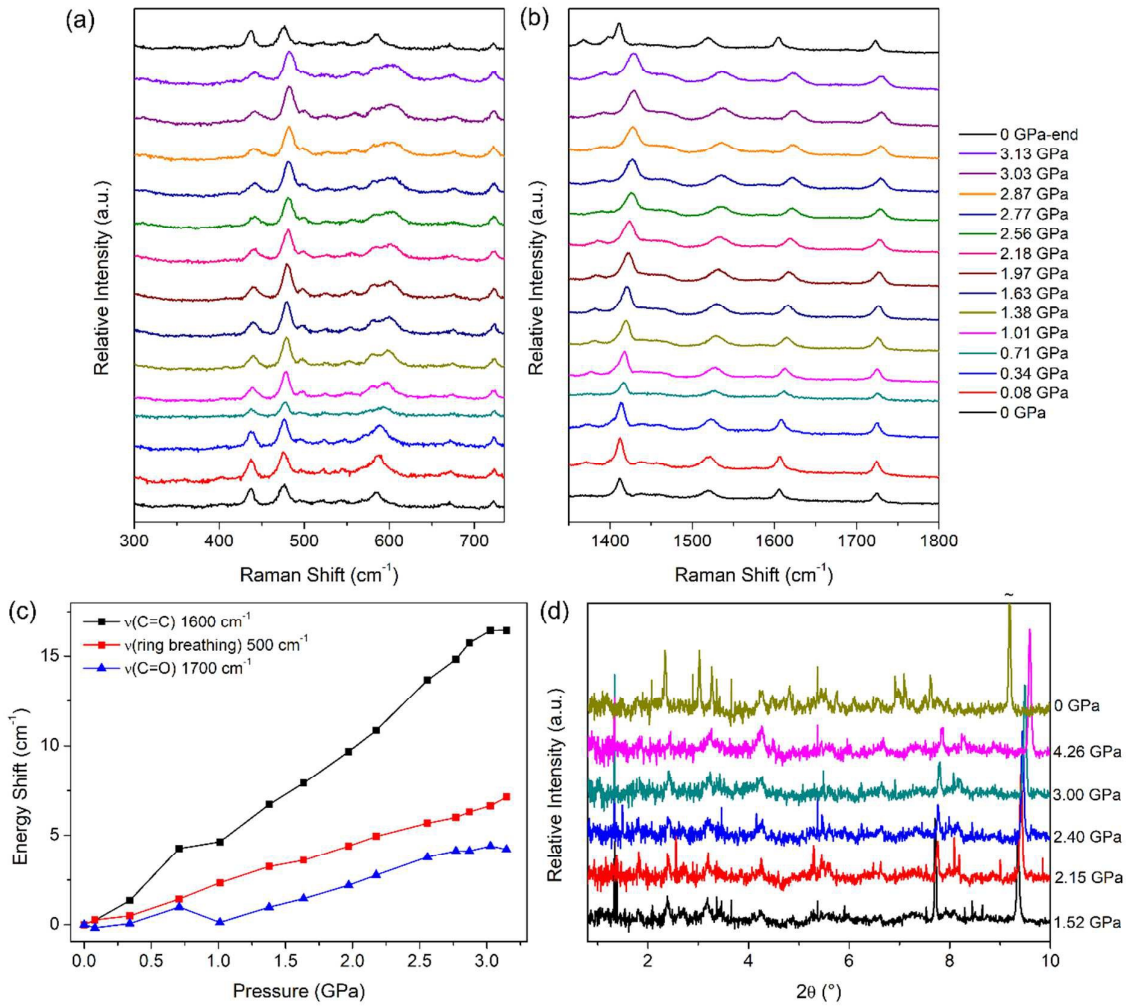

Figure 4. Pressure-dependent Raman spectroscopy of $[(Zn(DMF))_2(TTFTC)(DPNI)]$ under 632.8 nm laser excitation over the ranges (a) 300–740 cm^{-1} and (b) 1350–1800 cm^{-1}, (c) plot of energy shift in the Raman vibrational modes against applied pressure, (d) variable-pressure powder X-ray diffraction of $[(Zn(DMF))_2(TTFTC)(DPNI)]$ at multiple pressures where the pattern obtained at 0 GPa was collected following release of pressure from the system. The peak at approximately $2\theta = 9.5°$ is due to (200) of NaCl used as an internal pressure standard.

To complement the high pressure Raman spectroscopy study, variable pressure powder X-ray diffraction was performed to probe the structural changes incurred upon compression. As shown in Figure 4(d), at elevated pressures of 1.52–4.26 GPa, the crystallinity of the framework is significantly lower than at 0 GPa (achieved when pressure was released from

View Article Online
DOI: 10.1039/C8CP04157A

the system). This is commonly observed at applied pressures greater than the hydrostatic limit of the pressure medium (in this case Fluorinert FC-70), as freezing of the pressure medium results in sheer forces applying non-uniform pressure to the crystallites; this leads to peak broadening due to increased disorder in the system. Upon pressure release to 0 GPa, framework crystallinity was regained which demonstrates that the material is indeed stable to pressures up to 4.26 GPa. Rietveld analysis of the PXRD patterns revealed a slight but gradual contraction of the *a* and *b* axes, as well as a compression of the *β* angle (Table 1 and Figure S10). This is consistent with the monotonic blue shift of the Raman peaks with increasing pressure, whereby a contraction of the unit cell would result in a shortening of the ligand bonds. The repercussions of this contraction are likely to extend to a disruption of the charge transfer interaction in the way of orbital overlap and preference of the neutral states of TTFTC and DPNI (the central C=C bond of TTFTC and C=O bond of DPNI gain single bond character when in their radical states).

Table 1. Cell parameters of $[(Zn(DMF))_2(TTFTC)(DPNI)]$ and NaCl internal standard under applied pressure extracted by Rietveld analysis.

Pressure (GPa)	**NaCl (Å)**	***a***	***b***	***c***	***β***	**wRp-bkgd**
1.52	5.5444(8)	8.193(14)	20.13(15)	12.93(5)	91.9(6)	0.1103
2.15	5.5093(8)	8.139(10)	19.82(9)	12.93(4)	89.1(4)	0.0341
2.40	5.4914(8)	8.123(6)	19.71(6)	12.929(24)	86.03(22)	0.0682
3.00	5.4664(7)	8.118(13)	19.72(13)	12.88(5)	86.1(4)	0.0932
0	5.6459(19)	8.601(4)	20.771(23)	13.108(12)	94.47(8)	0.0293

CONCLUSIONS

In summary, the charge transfer complex between the redox-active TTFTC and DPNI ligands in the $[(Zn(DMF))_2(TTFTC)(DPNI)]$ framework was investigated using Raman spectroscopy and *in situ* Raman spectroelectrochemistry utilising a newly developed *in situ* method, as well as pressure-dependent Raman spectroscopy and PXRD. With the aid of DFT modelling, only the neutral forms of the ligands could be detected within the framework despite the DFT-calculated partial charge transfer of 0.6 e^- between TTFTC and DPNI units.[26] From this observation it can be concluded that the charge transfer is indeed heterogeneously distributed throughout the crystal lattice, possibly as a result of defects, giving rise to semiconductivity. Band structure calculations on the MOF confirmed that hole transport is the primary mechanism for charge migration. Upon oxidation, Raman bands corresponding to neutral

View Article Online
DOI: 10.1039/C8CP04157A

DPNI increased in intensity, whilst peaks due to neutral TTFTC concomitantly decreased, giving rise to the electrochemically-generated $TTFTC^{\bullet+}$–DPNI system whereby the charge on the DPNI ligand was predicted to be 0.2 e^- by DFT modelling.[26] The spectroscopic change associated with the redox transformation was found to be irreversible which was attributed to counter ion trapping inside the crystal lattice. From this study, it was shown that Raman SEC is an effective technique to assess redox state changes in porous solid state materials, which also provides insights into local structural changes. Pressure-dependent Raman and PXRD studies found a shortening of bond lengths associated with neutral TTFTC and DPNI – this is likely due to contributions from cell contraction as well as a decrease in the degree of D–A CT. Fundamental studies on the effects of external stimuli, such as pressure and redox modulation on the charge transfer characteristics of D–A MOFs will provide important insights into their potential as tuneable, switchable materials. These investigations are currently ongoing in our laboratory in regard to through space charge transfer interactions in a wide range of electroactive MOFs and CPs.[45]

Acknowledgements

We gratefully acknowledge support from Australian Research Council, SydneyNano and the Vibrational Spectroscopy Core Facility at the University of Sydney. O.K.F. gratefully acknowledges the support of the Nanoporous Materials Genome Center, funded by the U.S. DOE, Office of Science, Basic Energy Sciences Program (Award DE-FG02-17ER16362) J.T.H. acknowledges support from the U.S. Dept. of Energy, Office of Science, Office of Basic Energy Sciences (grant no. DE-FG02-87ER13808). TH acknowledges funding of Deutsche Forschungsgemeinschaft via the priority program COORNETS (SPP 1928, HE 3543/30-1).

REFERENCES

1. L. Sun, M. G. Campbell and M. Dincă, *Angew. Chem. Int. Ed.*, 2016, **55**, 3566-3579.
2. D. M. D'Alessandro, *Chem. Commun.*, 2016, **52**, 8957-8971.
3. D. M. D'Alessandro, J. R. R. Kanga and J. S. Caddy, *Australian Journal of Chemistry*, 2011, **64**, 718-722.
4. C. F. Leong, P. M. Usov and D. M. D'Alessandro, *MRS Bulletin*, 2016, **41**, 858-864.
5. J. N. Behera, D. M. D'Alessandro, N. Soheilnia and J. R. Long, *Chemistry of Materials*, 2009, **21**, 1922-1926.
6. L. E. Darago, M. L. Aubrey, C. J. Yu, M. I. Gonzalez and J. R. Long, *J. Am. Chem. Soc.*, 2015, **137**, 15703-15711.
7. P. Huo, T. Chen, J.-L. Hou, L. Yu, Q.-Y. Zhu and J. Dai, *Inorganic Chemistry*, 2016, **55**, 6496-6503.
8. V. Stavila, A. A. Talin and M. D. Allendorf, *Chem. Soc. Rev.*, 2014, **43**, 5994-6010.

View Article Online
DOI: 10.1039/C8CP04157A

9. K. T. Butler, C. H. Hendon and A. Walsh, *ACS Applied Materials & Interfaces*, 2014, **6**, 22044-22050.
10. H. Miyasaka, *Acc. Chem. Res.*, 2012, **46**, 248-257.
11. S. Goswami, D. Ray, K.-i. Otake, C.-W. Kung, S. J. Garibay, T. Islamoglu, A. Atilgan, Y. Cui, C. J. Cramer, O. K. Farha and J. T. Hupp, *Chem. Sci.*, 2018, **9**, 4477-4482.
12. C.-W. Kung, K. Otake, C. T. Buru, S. Goswami, Y. Cui, J. T. Hupp, A. M. Spokoyny and O. K. Farha, *J. Am. Chem. Soc.*, 2018, **140**, 3871-3875.
13. J. Ferraris, D. O. Cowan, V. Walatka and J. H. Perlstein, *Journal of the American Chemical Society*, 1973, **95**, 948-949.
14. J. B. Torrance, J. E. Vazquez, J. J. Mayerle and V. Y. Lee, *Phys. Rev. Lett.*, 1981, **46**, 253-257.
15. S. Matsuzaki, T. Moriyama and K. Toyoda, *Solid State Commun.*, 1980, **34**, 857-859.
16. D. Jankowski, R. Świetlik, O. Jeannin, A. Assaf, E. W. Reinheimer and M. Fourmigué, *Journal of Raman Spectroscopy*, 2013, **44**, 1765-1776.
17. R. Bozio, I. Zanon, A. Girlando and C. Pecile, *J. Chem. Phys.*, 1979, **71**, 2282-2293.
18. S. Matsuzaki, R. Kuwata and K. Toyoda, *Solid State Communications*, 1980, **33**, 403-405.
19. R. Bozio, A. Girlando and C. Pecile, *J. Chem. Soc., Faraday Trans. 2*, 1975, **71**, 1237-1254.
20. M. J. L. Santos, A. G. Brolo and E. M. Girotto, *Electrochimica Acta*, 2007, **52**, 6141-6145.
21. M. Kalbáč, L. Kavan, M. Zukalová and L. Dunsch, *Carbon*, 2007, **45**, 1463-1470.
22. R. S. Czernuszewicz and K. A. Macor, *Journal of Raman Spectroscopy*, 1988, **19**, 553-557.
23. D. L. Jeanmaire, M. R. Suchanski and R. P. Van Duyne, *Journal of the American Chemical Society*, 1975, **97**, 1699-1707.
24. I. Rey, J. C. Lassègues, P. Baudry and H. Majastre, *Electrochimica Acta*, 1998, **43**, 1539-1544.
25. R. P. Rava and T. G. Spiro, *The Journal of Physical Chemistry*, 1985, **89**, 1856-1861.
26. C. F. Leong, B. Chan, T. B. Faust and D. M. D'Alessandro, *Chem. Sci.*, 2014, **5**, 4724-4728.
27. M. Frisch, G. Trucks, H. Schlegel, G. Scuseria, M. Robb, J. Cheeseman, G. Scalmani, V. Barone, B. Mennucci and G. Petersson, *Gaussian Inc., Wallingford, CT*, 2009.
28. P. J. Stephens, F. J. Devlin, C. F. Chabalowski and M. J. Frisch, *The Journal of Physical Chemistry*, 1994, **98**, 11623-11627.
29. J. P. Merrick, D. Moran and L. Radom, *J. Phys. Chem. A*, 2007, **111**, 11683-11700.
30. L. Feketeova, G. N. Khairallah, B. Chan, V. Steinmetz, P. Maitre, L. Radom and R. A. J. O'Hair, *Chem. Commun.*, 2013, **49**, 7343-7345.
31. L. Feketeova, B. Chan, G. N. Khairallah, V. Steinmetz, P. Maitre, L. Radom and R. A. J. O'Hair, *Phys. Chem. Chem. Phys.*, 2015, DOI: 10.1039/c5cp01573a.
32. J. P. Perdew, K. Burke and M. Ernzerhof, *Physical Review Letters*, 1996, **77**, 3865-3868.
33. J. P. Perdew, M. Ernzerhof and K. Burke, *The Journal of Chemical Physics*, 1996, **105**, 9982-9985.
34. M. F. Peintinger, D. V. Oliveira and T. Bredow, *Journal of Computational Chemistry*, 2013, **34**, 451-459.
35. R. Dovesi, R. Orlando, A. Erba, C. M. Zicovich-Wilson, B. Civalleri, S. Casassa, L. Maschio, M. Ferrabone, M. De La Pierre, P. D'Arco, Y. Noël, M. Causà, M. Rérat and B. Kirtman, *International Journal of Quantum Chemistry*, 2014, **114**, 1287-1317.
36. K. J. Reszka, M. Takayama, R. H. Slk, C. F. Chignell and I. Salto, *Photochem. Photobiol.*, 2005, **81**, 573-580.
37. M. Giffard, P. Alonso, J. Garín, A. Gorgues, T. P. Nguyen, P. Richomme, A. Robert, J. Roncali and S. Uriel, *Adv. Mater.*, 1994, **6**, 298-300.
38. L. Sun, S. S. Park, D. Sheberla and M. Dincă, *J. Am. Chem. Soc.*, 2016, **138**, 14772-14782.
39. Y. Singh, *AIP Conf. Proc.*, 2016, **1728**, 020692.
40. M. Cointe, E. Collet, B. Toudic, P. Czarnecki and H. Cailleau, *Crystals*, 2017, **7**, 285.
41. S. C. McKellar and S. A. Moggach, *Acta Crystallogr. Sect. B*, 2015, **71**, 587-607.
42. J. Yang, L. Zhou, J. Cheng, Z. Hu, C. Kuo, C.-W. Pao, L. Jang, J.-F. Lee, J. Dai, S. Zhang, S. Feng, P. Kong, Z. Yuan, J. Yuan, Y. Uwatoko, T. Liu, C. Jin and Y. Long, *Inorg. Chem.*, 2015, **54**, 6433-6438.

View Article Online
DOI: 10.1039/C8CP04157A

43. M. Andrzejewski and A. Katrusiak, *The Journal of Physical Chemistry Letters*, 2017, **8**, 929-935.
44. G. Mehlana and S. A. Bourne, *CrystEngComm*, 2017, **19**, 4238-4259.
45. C. Hua, P. W. Doheny, B. Ding, B. Chan, M. Yu, C. J. Kepert and D. M. D'Alessandro, *J. Am. Chem. Soc.*, 2018, **140**, 6622-6630.

View Article Online
DOI: 10.1039/C8CP04157A

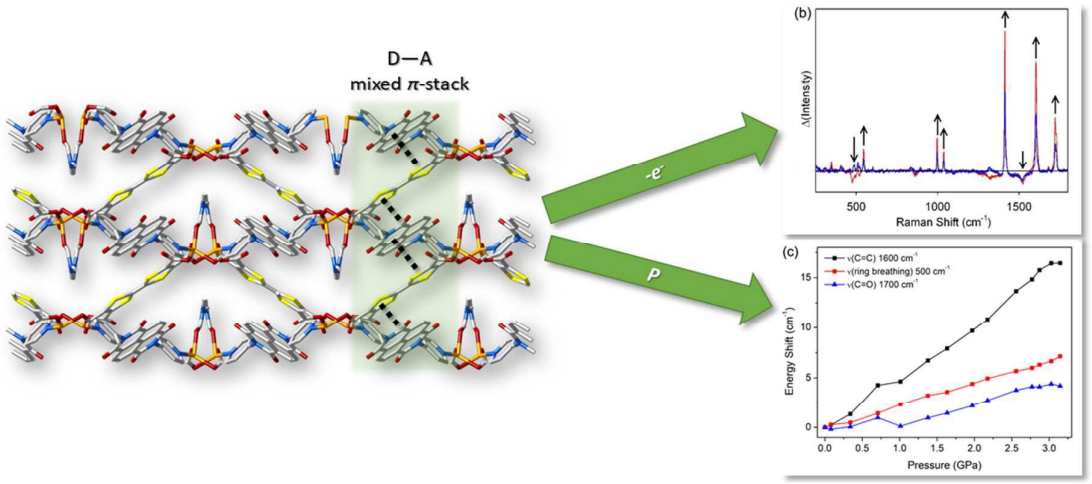

Donor-Acceptor Metal-Organic Frameworks display redox and pressure dependent charge transfer properties.